Joint International Topical Meeting on Mathematics & Computation and Supercomputing in Nuclear Applications (M&C + SNA 2007)
Monterey, California, April 15-19, 2007, on CD-ROM, American Nuclear Society, LaGrange Park, IL (2007)

APPLICATION OF NODAL EQUIVALENCE PARAMETERS TO PRISMATIC VHTR CORE ANALYSIS

C. H. Lee, Z. Zhong, T. A. Taiwo, and W. S. Yang
Argonne National Laboratory
9700 South Cass Avenue, Argonne, IL 60439, USA
clee@anl.gov

H. K. Joo
Korea Atomic Energy Research Institute
150 Deokjin-dong, Yuseong-gu, Daejeon, Korea
hkjoo@kaeri.re.kr

ABSTRACT

The generation of nodal cross sections and equivalence parameters for prismatic VHTR core components is discussed. For fuel-block cross section generation, a conventional single-block model with a reflective boundary condition is used. A one-dimensional fuel-reflector model is proposed for reflector cross section generation in order to accurately represent the significant neutron spectrum variation at the core-reflector interface. Two-dimensional multi-block models are used for obtaining control rod cross sections for rodded fuel and reflector blocks to best approximate actual spectra in the blocks. The verification of the models was performed by generating cross sections with the DRAGON and HELIOS codes, using the cross section data in 2-D and 3-D DIF3D nodal calculations, and comparing the results to MCNP4C ones. The results show that the use of discontinuity factors reduces errors in nodal solutions for the multiplication factor and power distribution. Surface-dependent discontinuity factors are found essential for improving the accuracy of the power distribution of cores with asymmetrically rodded blocks when nodal calculations are performed with one node per hexagonal block.

Key Words: Prismatic VHTR, equivalence theory, discontinuity factors, nodal solution

1. INTRODUCTION

The prismatic Very High Temperature Reactor (VHTR) is one of the leading candidates for the Next Generation Nuclear Plant (NGNP) [1] in the U.S. The double heterogeneity of VHTR fuel elements caused by the use of coated fuel particles is one of the distinct characteristics that have to be properly treated in neutronics analysis. An annular core design makes neutron leakage into the inner and outer reflectors more important than in traditional light water reactors (LWRs) because high power peaks occur at the core-reflector interfaces. Large local flux variations near the core-reflector interface require accurate reflector cross sections to preserve the reaction rates in the reflector and the leakage at the interface. Furthermore, control rods are designed to be inserted in a sixth-sector of hexagonal blocks in the fuel and reflector regions; e.g., operating control rods in reflector regions and startup or shutdown control rods in fuel regions. It is therefore challenging to obtain control rod cross sections in the rodded reflector and fuel blocks because of the asymmetric intra-block geometry and significant heterogeneity effects. Due to these factors, the cross sections of individual components (fuel block, reflector, control rod,

burnable poisons, etc.) should be properly generated in lattice physics calculations in order to accurately model prismatic VHTR cores.

In this paper, approaches are presented for generating cross sections for use in deterministic nodal codes. Nodal equivalence parameters (discontinuity factors) [2] typically employed in advanced nodal methods for LWR cores are introduced to reduce homogenization errors arising from VHTR core heterogeneity. The use of surface-dependent discontinuity factors for improving the solution accuracy of rodded cores is discussed. To demonstrate the performance of those cross sections, mini-core and 2-D and 3-D core calculations are performed for various conditions with control rods and burnable poisons.

The DRAGON [3] and HELIOS [4] lattice physics codes have been used for cross section generation. It is noted that the DRAGON code has a capability to model coated fuel particles explicitly at the assembly level but the multi-block modeling capability is limited, whereas the HELIOS code has better capabilities for multi-block lattice calculations but cannot model particulate fuels. The diffusion theory approximation of the VARIANT nodal transport capability of the DIF3D code [5] has been employed for core calculations.

2. CROSS SECTION GENERATION BASED ON NODAL EQUIVALENCE THEORY

The nodal equivalence theory has been found to be very effective for estimating the high-order heterogeneous solution by solving the corresponding low-order homogenous equation with additional parameters (discontinuity factors) introduced to preserve reaction rates, average fluxes, and average leakages of the higher-order solution. Since the neutron spectrum variation is significant at the fuel-reflector interface of VHTR cores, discontinuity factors (DFs) could be very useful for preserving currents at the interface. In addition, surface-dependent DFs make it possible to preserve all surface currents of a geometrically asymmetric block with a single-set of homogenized cross sections. In this section, cross section generation approaches for VHTR components are discussed.

2.1. Fuel Block Cross Sections

In the current study, the VHTR fuel block cross sections are obtained from lattices physics calculations using a single-block model with a reflective boundary condition, as is typically done in light water reactor analysis. The discontinuity factors are simply calculated as the ratio of the surface-average and block-average fluxes. The group constants and equivalence parameters determined from this single fuel block calculation would be adequate provided the actual spectrum in the core is not significantly different from that of the single fuel block.

Figure 1 shows DFs obtained from the DRAGON calculations for fuel blocks with and without burnable poisons (BPs) or control rods (CRs). In this study, burnable poisons are assumed loaded in the six corner holes of a fuel block and a control rod is located in one of the six sectors of the fuel block. For comparison purposes, a case with control rod placed at the center of a fuel block is also evaluated, although the actual position is in a sixth-sector of hexagonal block.

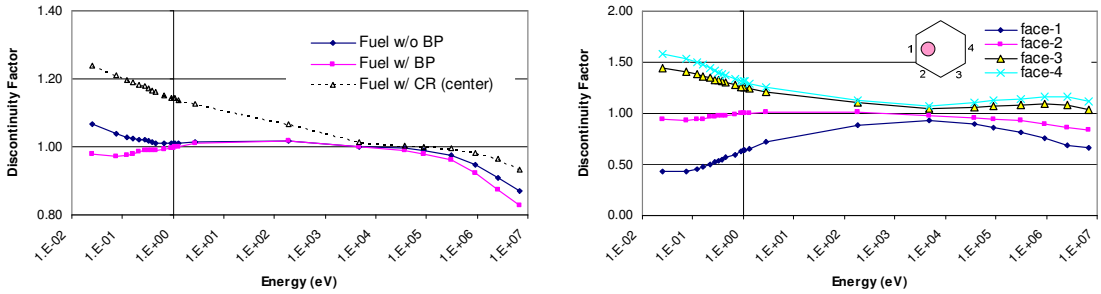

Figure 1. Discontinuity Factors (23-group) of Fuel Blocks with/without BP or CR.

For a fuel block, the fast group DFs are smaller than unity because fast group fluxes at the peripheral graphite region are smaller than the block average fluxes. The thermal group DFs are larger than unity due to increased neutron thermalization in the boundary region. For a fuel block with BPs, however, thermal group fluxes at the block boundary are smaller than the block average ones due to the flux depression caused by BPs at the six corner holes. As indicated, the DFs of a fuel block containing a central control rod are significantly different from unity in the thermal and epithermal energy regions, compared to those of an unrodded fuel block. The surface-dependent DFs of an asymmetrically rodded fuel block have very distinct values for each surface due to the asymmetric loading of a strong absorber. This observation implies that the surface discontinuity effects are not negligible for unrodded fuel blocks and are very significant for rodded fuel blocks. The generation of cross sections for the rodded fuel block will be revisited in Section 2.3.

2.2. Reflector Cross Sections

Few-group reflector cross sections significantly vary with distance from the interface between the core and reflector regions because the thermal neutron spectrum changes substantially at the fuel-reflector interface. The application of discontinuity factors would make it possible to use a single-set of cross sections for each of the inner, outer, and axial reflector regions with good accuracy. Thus, one-dimensional (1-D) models illustrated in Figure 2 are proposed for generating radial reflector cross sections.

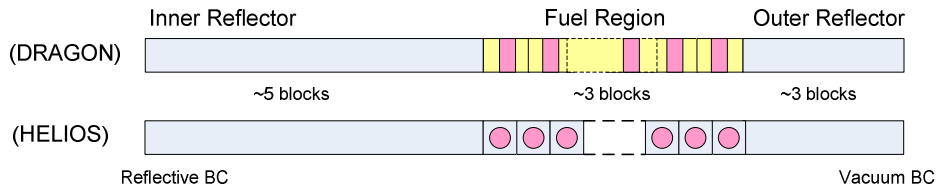

Figure 2. One-Dimensional Fuel-Reflector Model.

For DRAGON, the hexagonal pin-cell geometry is converted to a slab-cell, maintaining the same neutronics characteristics, whereas for HELIOS, it is changed to a rectangular pin-cell one (choices dictated by accuracy of code capabilities). A reflective boundary condition is employed for the inner reflector boundary and a vacuum boundary condition for the outer reflector boundary. Discontinuity factors at the interface between the fuel and reflector are derived

dividing the heterogeneous surface fluxes of the DRAGON or HELIOS solution by the homogenous surface fluxes obtained from a finite difference method (FDM) solution with boundary current sources.

2.3. Control Rod Cross Sections

In prismatic VHTR cores, control rods are inserted in reflector blocks for regulating purposes during operation and in fuel blocks for startup and shutdown purposes. For obtaining cross sections for a rodded reflector block, a two-dimensional (2-D) multi-block model with a reflective boundary condition is proposed. As illustrated in Figure 3(a), the model consists of a rodded reflector block surrounded by 3 fuel and 3 reflector blocks.

Using the homogenized cross sections and boundary current sources of the rodded reflector block from the multi-block calculation, the homogenous surface fluxes were obtained from FDM calculations. These heterogeneous and homogeneous surface fluxes are used to determine discontinuity factors for all surfaces of the rodded block.

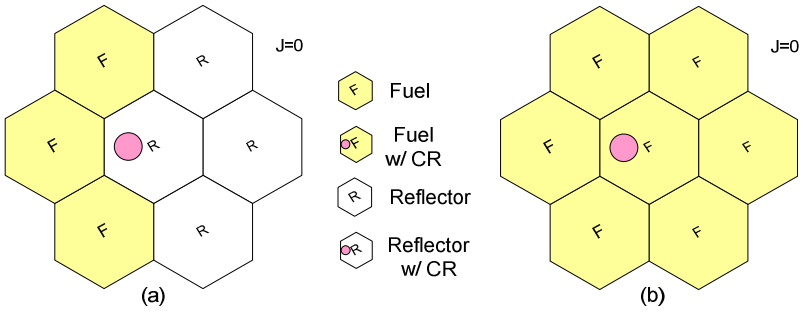

Figure 3. Two-Dimensional Multi-Block Models for Control Rods.

For a fuel block containing a control rod loaded asymmetrically, a preliminary study showed that the use of homogenized cross sections and DFs generated using a single-block model leads to a higher rodded fuel block power and lower control rod worth compared to MCNP4C [6] reference values. This is because the thermal flux depression in the rodded sector is exaggerated with the reflective boundary condition of the single block model, resulting in lower absorption cross sections. It is noted that the control rod pattern of the VHTR core does not have rodded sectors of neighboring blocks facing each other and hence the reflective boundary condition cannot be applied. Therefore, it is imperative to use a multi-block calculation for a rodded fuel block, as shown in Figure 3(b), in order to obtain more realistic homogenized cross sections and equivalence parameters for rodded fuel blocks. The surface-dependent discontinuity factors for the rodded fuel block are calculated in the same manner as discussed for the rodded reflector block above.

3. VERIFICATION TESTS

The adequacy of the approaches proposed for generating nodal cross sections and equivalence parameters has been tested with 2-D and 3-D core cases as well as the following seven-block mini-core cases:

- Case BP-1: BP fuel block located at the center of the model,

- Case BP-2: BP fuel block located at the periphery of the model,
- Case CR-F1: CR (center) fuel block located at the center of the model,
- Case CR-F2: CR (center) fuel block located at the periphery of the model,
- Case CR-F3: CR (asymmetric position) fuel block located at the center of the model (see Figure 3(b)),
- Case CR-R: CR (asymmetric position) reflector block located at the center of the model (see Figure 3(a)).

The cases BP-1, BP-2, CR-F1 and CR-F2 contain all symmetric blocks, whereas the cases CR-F3 and CR-R have a block with a control rod loaded in an asymmetric position.

The 2-D core cases that have been tested include the cases with CR inserted in the reflector or fuel region as well as the cases without CR. For simplicity, locations of blocks with BP or CR were chosen to give one-twelfth core symmetry. A 3-D core calculation was also performed for the case without CR and BP to compare the axial power distribution.

Utilizing the approaches discussed in the previous section, cross sections and discontinuity factors for fuel and reflector were obtained from DRAGON and HELIOS calculations. Group constants for control rods in fuel and reflector regions were obtained only from HELIOS calculations since DRAGON does not allow explicit modeling of multiple hexagonal blocks. With DRAGON, 23-group cross sections were generated using the 172-group library at 300 K; with HELIOS, 20-group cross sections with the 190-group library. In the lattice codes, the control rod in the fuel or reflector block was approximated with three hexagonal-cell rings as shown in Figure 4.

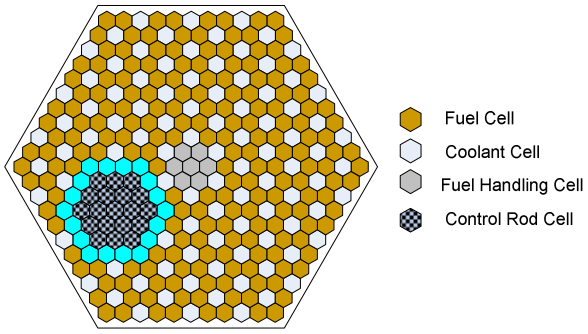

Figure 4. Control Rod Configuration in Fuel Block.

Core calculations were performed using the VARIANT [7] variational nodal transport option of the DIF3D code. This option uses a hybrid finite element method that guarantees nodal balance and permits refinement through the use of hierarchical complete polynomial trial functions in space and spherical harmonics or simplified spherical harmonics in angle. It has been shown that the diffusion theory solution (P_1 angular flux approximation) of VARIANT is more accurate than the nodal diffusion capability of the DIF3D code. In this study, only the P_1 approximation of the VARIANT option was used in order to utilize the nodal equivalence parameters. One node per hexagonal block was used in the calculations.

The multiplication factors (k_{inf}) of fuel blocks at 300 K calculated using the DRAGON and HELIOS codes have been compared with those from the MCNP4C code. Cross section libraries for all codes are based on ENDF/B-VI data. Results are presented in Table I. It is found that the double heterogeneity effect of using coated fuel particle (TRISO) in a graphite matrix is 2.4 ~ 3.0% $\Delta\rho$ (this is the reactivity difference between the results for homogeneous compact and explicit TRISO particle models). It is also observed that the k_{inf} calculated by DRAGON for the case employing the explicit TRISO particle representation is about ~0.5% $\Delta\rho$ higher than the MCNP4C solution. Therefore, for subsequent verification tests in this paper, the homogeneous fuel compact has been used to eliminate errors arising from the treatment of the double heterogeneity effect in the deterministic code.

Table I. Comparison of k_{inf} Values from MCNP4C, DRAGON, and HELIOS for Fuel Block.

Fuel Type	Block Type	MCNP4C [a)]	DRAGON	HELIOS
Homogeneous Fuel Compact	No-BP	1.4743	1.4752	1.4766
	BP	1.2078	1.2098	1.2116
Explicit TRISO Particles	No-BP	1.5291	1.5406	-
	BP	1.2525	1.2613	-

a) Standard deviation of MCNP4C results ≤ 0.00031

Results for the mini-core cases are summarized in Table II. Cross sections and equivalence parameters for cases BP-1, BP-2, CR-F1, and CR-F2 were generated using the DRAGON single-block model. Those for cases CR-F3 and CR-R including rodded fuel or reflector blocks were obtained from HELIOS calculations since, as aforementioned, cross sections and surface-dependent DFs for rodded blocks were derived from multi-block models.

Table II. Differences between MCNP4C and DIF3D Multiplication Factor, Power, and Control Rod Worth for Mini-Cores.

Case	MCNP4C Eigenvalue [a)]	DIF3D					
		w/o DF			w/ DF		
		% $\Delta\rho$	Max Power, %	CR Worth, %	% $\Delta\rho$	Max Power, %	CR Worth, %
BP-1 [b)]	1.42957	0.310	-3.2	-	0.211	0.3	-
BP-2 [b)]	1.43467	0.173	-1.8	-	0.102	1.0	-
CR-F1 [b)]	1.33365	-1.248	11.2	13.8	-0.459	1.3	5.4
CR-F2 [b)]	1.36702	-0.938	11.2	13.8	-0.477	3.6	7.3
CR-F3 [c)]	1.33531	-0.399	13.3	7.1	0.179	1.6	-1.1
CR-R [c)]	1.17841	1.208	11.1	-15.1	-0.572	6.2	0.2

a) Standard deviation of MCNP4C results ≤ 0.00031
b) Cross sections obtained from DRAGON calculations
c) Cross sections obtained from HELIOS calculations

The comparison of DIF3D and MCNP4C results for the mini-core cases show that by using DFs in DIF3D calculations the discrepancies in multiplication factor, power, and control rod worth

are reduced for all the cases. Maximum power error is significantly reduced, especially for the cases with control rod. The results for cases BP-1, BP-2, CR-F1 and CR-F2 indicate that the fuel block DFs generated using a single-block model work well. In addition, the results for cases CR-F3 and CR-R show that surface-dependent DFs are required to obtain accurate power distributions for asymmetrically rodded cases.

Table III is a summary of the differences in the core multiplication factor, power, and control rod worth between MCNP4C and DIF3D for the 2-D core cases. For unrodded cores, DRAGON and HELIOS were used to generate the cross sections, whereas only the HELIOS code was employed for generating cross sections of rodded cores, which require multi-block calculations. The locations of rodded blocks (CA, CB, and SA in Table III) can be found in Figures 7 and 8. As shown in the table, multiplication factor and power are improved for all cases using DFs. In particular, the improvement was significant for the cores with control rods.

Table III. Differences between MCNP4C and DIF3D Multiplication Factor, Power, and Control Rod Worth for 2-D Core Cases.

Core Configuration		MCNP4C Eigenvalue [a]	w/o DF			w/ DF		
			% Δρ	Power, % (Max / RMS)	CR Worth, %	% Δρ	Power, % (Max / RMS)	CR Worth, %
			DRAGON / DIF3D					
No-BP/CR		1.39689	0.083	2.6/1.3	-	-0.240	1.3/0.8	-
BP		1.31077	0.626	-3.1/1.5	-	0.290	2.3/1.1	-
			HELIOS / DIF3D					
No-BP/CR		1.39689	0.363	1.2/0.6	-	0.080	1.1/0.5	-
BP		1.31077	0.954	-3.7/1.5	-	0.657	-1.5/0.8	-
CR in Reflector	CA in	1.36657	0.215	8.9/3.0	-8.5	0.143	-3.2/1.4	-4.0
	CB in	1.31420	1.384	12.3/5.5	-29.9	0.387	-4.4/1.7	-6.8
	CA+CB in	1.29528	1.508	14.8/6.7	-25.4	0.637	5.3/2.3	-9.9
CR in Fuel	SA in	1.22495	1.610	12.9/7.0	-15.2	0.291	-4.7/2.1	-2.1

a) Standard deviation of MCNP4C results ≤ 0.00037

Figures 5 to 8 display power distributions from MCNP4C and DIF3D calculations for the 2-D core cases ($1/12^{th}$ sector shown). Compared to the MCNP4C solutions, maximum power discrepancies of HELIOS/DIF3D are 1.5% for unrodded cores and 5.3% for rodded cores. Maximum percent power differences in the rodded cores occur in the fuel blocks with low power (see Figures 7 and 8). The comparison between MCNP4C and DIF3D solutions indicates that the use of surface-dependent DFs improves the accuracy of the power distribution. As shown in Figures 7 and 8, the combination of homogenized cross sections and surface-dependent discontinuity factors corrects the power tilt around the rodded blocks arising from the asymmetric loading of control rod.

Similarly to the 2-D core results, those from DIF3D for the 3-D core (actual core height of 793 cm and the same top and bottom reflector size of 120 cm) are also in good agreement with MCNP4C solutions: multiplication factor difference of -0.29% Δρ and maximum and RMS power differences of -1.2% and 0.5%, respectively. Figure 9 compares axial power distributions from MCNP4C and DRAGON/DIF3D and shows that they are in very good agreement.

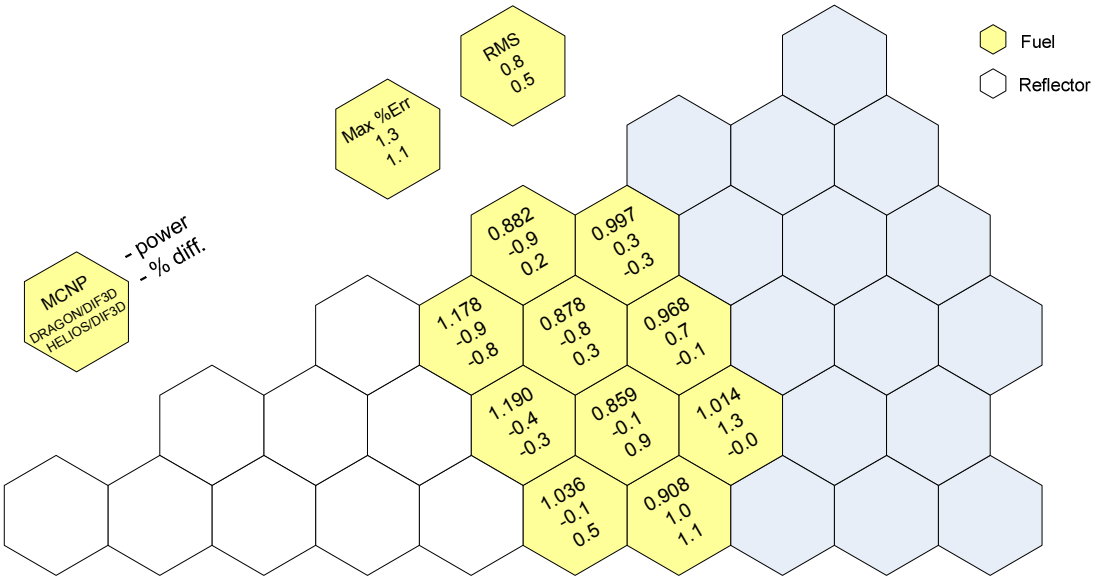

< % diff. = (DIF3D – MCNP) / MCNP * 100 >

Figure 5. Power Distributions from MCNP4C and DIF3D for 2-D Core.

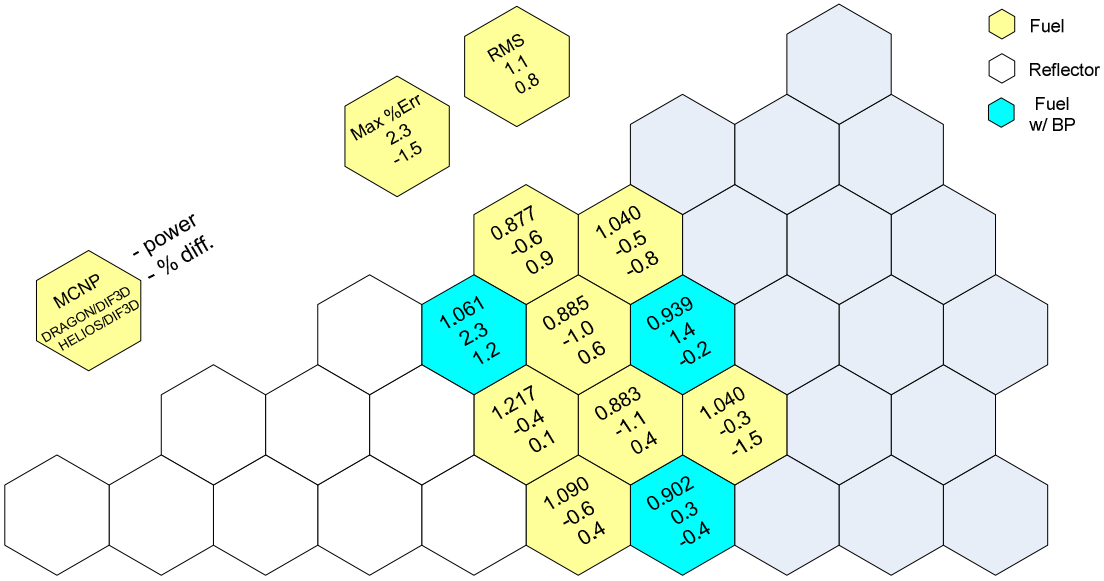

< % diff. = (DIF3D – MCNP) / MCNP * 100 >

Figure 6. Power Distributions from MCNP4C and DIF3D for 2-D Core with BPs.

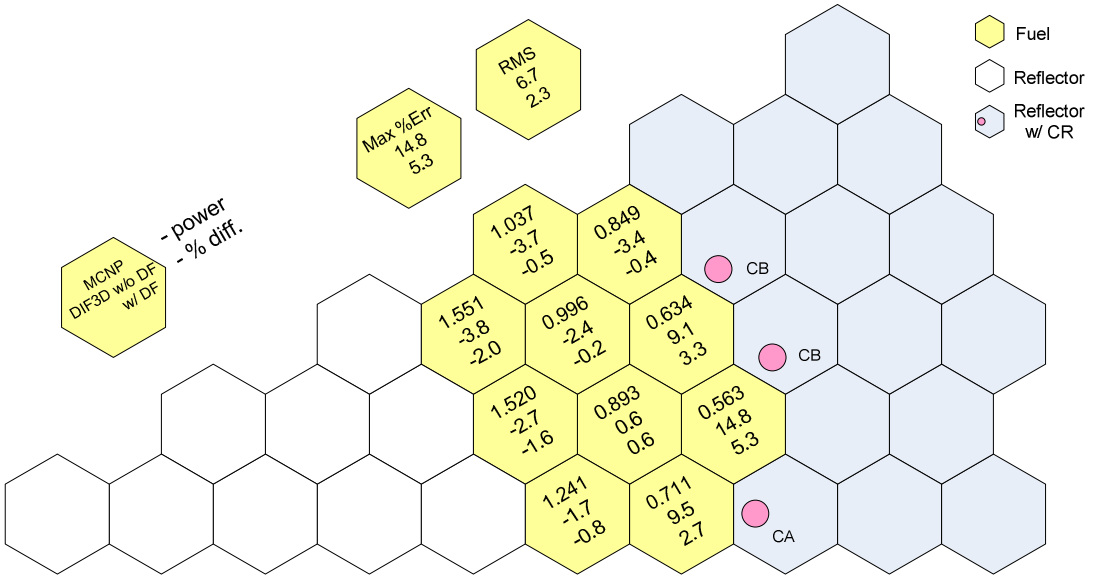

< % diff. = (DIF3D – MCNP) / MCNP * 100 >

Figure 7. Power Distributions from MCNP4C and HELIOS/DIF3D for 2-D Core with Control Rods in the Reflector Block.

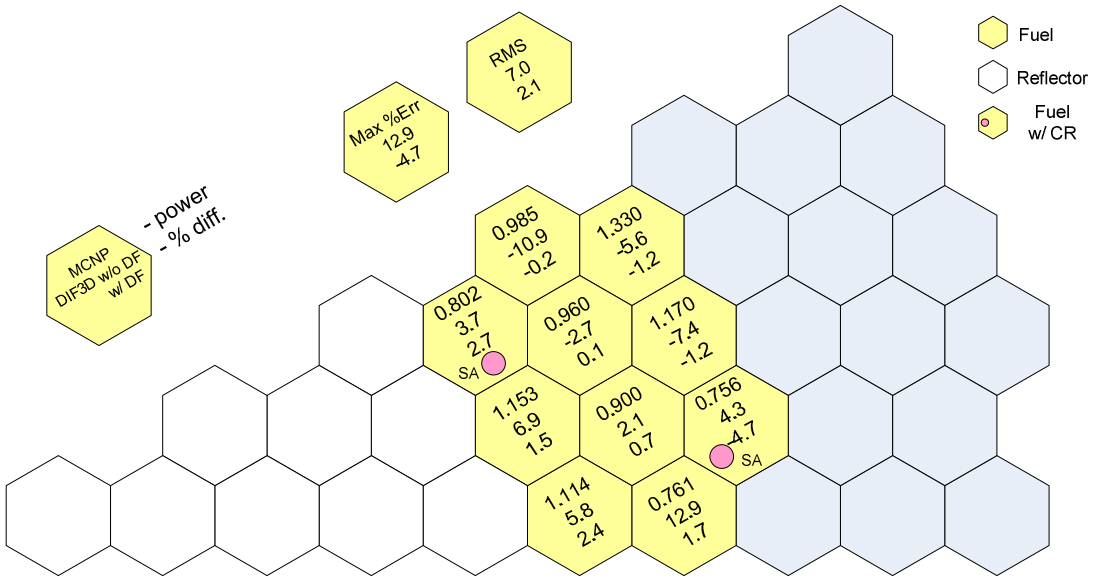

< % diff. = (DIF3D – MCNP) / MCNP * 100 >

Figure 8. Power Distributions from MCNP4C and HELIOS/DIF3D for 2-D Core with Control Rods in the Fuel Block.

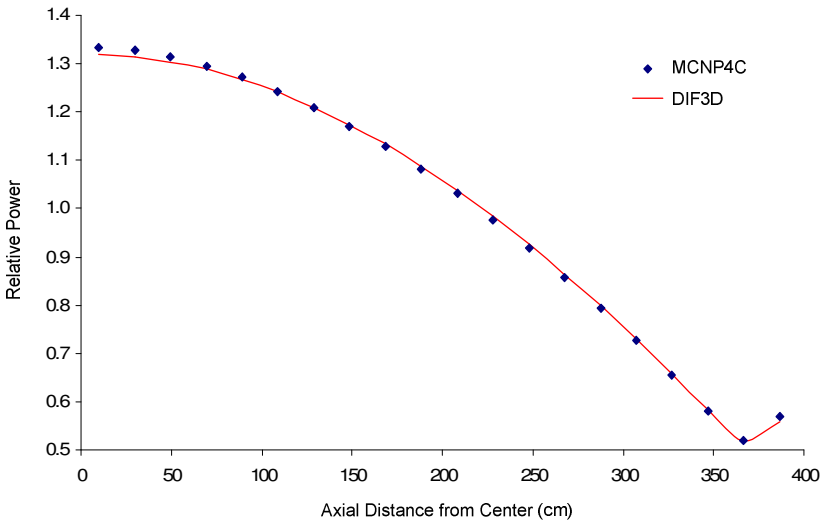

Figure 9. Axial Power Distributions from MCNP4C and DRAGON/DIF3D for 3-D Core.

4. CONCLUSIONS

The approaches for the generation of cross sections and equivalence parameters for core nodal calculations of prismatic VHTR cores have been discussed. Equivalence parameters are applied to accurately account for the significant variation of the neutron spectrum at the interface of fuel and reflector regions as well as the regions containing strong absorbers. Surface-dependent discontinuity factors (DFs) are utilized to best account for control rods asymmetrically positioned in fuel or reflector blocks. This is required to obtain good accuracy when one node per hexagonal block is used for core calculations.

Cross sections and DFs for fuel blocks are generated using a single-block model with reflective boundary conditions. Reflector cross sections are obtained with a 1-D fuel-reflector model. For generating accurate cross sections in rodded fuel and reflector regions, a multi-block model has been found essential to improve the accuracy of the core reactivity and power distribution.

The results from mini-core and 2-D and 3-D core calculations indicated that the application of DFs improves the estimation of multiplication factors and powers. Power distribution discrepancies arising from asymmetric loading of control rod were significantly reduced by using surface-dependent DFs.

The use of triangular nodes instead of one hexagonal node might relieve the necessity of surface-dependent discontinuity factors. Additionally, the control rod reactivity could be more effectively estimated by taking into account the spectrum condition surrounding the rodded triangular node. In the future, triangular based calculations will be evaluated, incorporating equivalence parameters into cross sections.

ACKNOWLEDGMENTS

This work was supported by the U.S. Department of Energy under Contract number DE-AC02-06CH11357.

REFERENCES

1. T. K. Kim, W. S. Yang, T. A. Taiwo, and H. S. Khalil, "Equilibrium Cycle Analysis in Support of Fuel Specification for Next Generation Nuclear Power Plants," *2005 International Congress on Advances in Nuclear Power Plants*, May 15-19, Seoul, Korea (2005).
2. K. S. Smith, "Spatial Homogenization Methods for Light Water Reactor Analysis," Ph.D. Thesis, Massachusetts Institute of Technology (1980).
3. G. Marleau, et al., "A User Guide for DRAGON," Technical report IGE-174 Rev. 4, Ecole Polytechnique de Montréal (1998).
4. R. J. Stamml'er et al., "HELIOS Methods," Studsvik Scanpower (1998).
5. R. D. Lawrence, "The DIF3D Nodal Neutronics Option for Two- and Three-Dimensional Diffusion Theory Calculations in Hexagonal Geometry," ANL-83-1, Argonne National Laboratory (1983).
6. J. F. Briesmeister, el al., "MCNP^{TM} - A General Monte Carlo N-Particle Code, Version 4C," LA-13709-M, Los Alamos National Laboratory (2000).
7. G. Palmiotti, E. E. Lewis, and C. B. Carrico, "VARIANT: VARIational Anisotropic Nodal Transport for Multidimensional Cartesian and Hexagonal Geometry Calculation," ANL-95/40, Argonne National Laboratory (1995).